International Journal of Earth, Energy and Environmental Sciences
ISSN: 2517-942X
Vol:11, No:9, 2017

Image Processing on Geosynthetic Reinforced Layers to Evaluate Shear Strength and Variations of the Strain Profiles

S. K. Khosrowshahi, E. Güler

***Abstract*—**This study investigates the reinforcement function of geosynthetics on the shear strength and strain profile of sand. Conducting a series of simple shear tests, the shearing behavior of the samples under static and cyclic loads was evaluated. Three different types of geosynthetics including geotextile and geonets were used as the reinforcement materials. An image processing analysis based on the optical flow method was performed to measure the lateral displacements and estimate the shear strains. It is shown that besides improving the shear strength, the geosynthetic reinforcement leads a remarkable reduction on the shear strains. The improved layer reduces the required thickness of the soil layer to resist against shear stresses. Consequently, the geosynthetic reinforcement can be considered as a proper approach for the sustainable designs, especially in the projects with huge amount of geotechnical applications like subgrade of the pavements, roadways, and railways.

***Keywords*—**Image processing, soil reinforcement, geosynthetics, simple shear test, shear strain profile.

I. Introduction

THE efficiency of geosynthetics in the geotechnical engineering applications and the related disciplines has been successfully approved by several researches and projects. Regarding different projects and the desired properties, geosynthetics are applicable with various functions. The reinforcement feature, can be remarked as one of the major functions of geosynthetics. A geosynthtic-reinforced soil, is a material which is combined the tensile strength of geosynthetic and the high compression strength of soil. In addition to the tensile strength, a proper geometry and material toughness can increase the friction between soil and geosynthetic, and consequently improve the shear strength. There is a widespread use of the geosyntheic reinforcement in various geotechnical and earth work applications such as embankments, retaining structures, slope stability, and improvement the subgrade of pavements, roadways, and railways. In addition to the shear failure, considering the serviceability and for keeping a project on the safe side, it is required to eliminate the displacements according to the corresponding specifications for each project. In this study, it is shown that beside the enhancement of the shear strength, the geosynthetic reinforcement also reduces the shear strains effectively.

It is aimed to investigate the effect of the geosynthetic reinforcement on the shear strength of a sand layer under static and cyclic loads and also to determine the shear strain profiles by use of image processing analysis. The idea is to obtain a relation between the implementing different reinforcement materials and the changes of the shear strains along the height of the samples.

S. K. Khosrowshahi and E. Güler are with the Civil Engineering Department, Bogazici University, Bebek, 34342, Istanbul, Turkey (e-mail: samad.kazemi@boun.edu.tr, eguler@boun.edu.tr).

II. Geosynthetic Reinforcement and Image Processing on Geotechnical Engineering

In geotechnical engineering, reinforcement is known as a beneficial technique for improving the engineering properties of the weak or problematic soils instead of some conventional methods, such as increased layers or replacing the in-situ materials by the soils with the desired strength. Consequently, it leads to a more sustainable design and decreases the costs and CO_2 emission which are generated by the huge amount of works for soil replacing and transportation in the typical approaches. According to the literature, geosynthetics have been widely used in different projects for enhancing the efficiency of geosystems. Separation, filtration, drainage, and reinforcement can be mentioned as the main functions of the geosynthetics. Many studies approve the effect of geosynthetic reinforcement on improving the strength properties on the railway subgrade construction [1]-[3]. Geotextile and geogrid are two types of the geosynthetics with a satisfied reinforcement function. Several researchers have investigated the reinforcement mechanisms of geogrids associated with the interaction of geogrids and unbound aggregate. The most applications of geogrids involve placing a singular layer within or at the bottom of the base or subbase granular fill [4], [5]. In 2017, Güler and Khosrowshahi conducted a series of simple shear tests on the sand samples reinforced by geotextile and geogrid. They observed the enhancement of the shear strength under the static and cyclic shearing loads [6]. Ashmawy and Bourrdeau studied the effect of geotextile reinforcement on the stress-strain and volumetric behavior of sand under monotonic and cyclic loads. The results revealed a significant increase in monotonic shear strength and ductility of sand with a reduction in cyclic deformability [7]. Broms by conducting a triaxial tests on the samples which geotextile which was placed horizontally, showed a reduction in the lateral earth pressure of geotextile-reinforced sand [8]. Also, some researches carried out to investigate the influence of the use of geosynthetics on reduction of the required thickness of subgrades in pavements and roadways.

Hufenus et al., performed a full-scale field test on a

geosynthetic reinforced unpaved road considering compaction and trafficking, to evaluate the bearing capacity and its performance on a soft subgrade. The results approved a reduction in the thickness of the fill layer for the certain values of compaction and bearing capacities, and also a reduction in the rut formation as a function of the trafficking [9]. Ziaie and Nazari investigated the effect of geotextile and geogrid on the road constructions. They performed a series of the CBR tests on two layered soil consisting of a granular soil on top as the subbase layer and a soft clayey soil at bottom as subgrade layer. The results showed an increase in compression strength of the reinforced specimens. Comparing with geotextiles, geogrids were more efficient on improving strength due to the interlocking with the subbase layer aggregates [10].

Image processing is represented as a new and useful technique in geotechnical engineering. It is considered as a proper approach for observing displacements and measuring the deformations which occur over a long period of time. Several studies reveal the use of image processing in the characterization of soil fabric [11]-[15]. These studies investigate the shearing behavior of the soil microstructure. Several similar methods have also been applied to evaluate the pattern of soil deformation during shear. Alshibli and Sture [16], [17] applied a grid on the triaxial membrane to study on the shear profile formation without using tracing markers. Harris et al. [18] and Finno et al. [19] benefited the stereo photogrammetry into investigating the deformation associated with shear banding in granular soil.

In this study, by using MATLAB codes, the shear strain profiles were determined. The used method is based on the measurement of the displacements between the frames of the initial and deformed samples.

III. Experimental Procedure

The experimental program involves three main parts: I) Direct simple shear tests (DSS) for static loads, II) Cyclic simple shear tests (CSS) for cyclic loads, III) Image processing analysis on the DSS tests to explore the effect of the reinforcement on reduction of the lateral displacements.

The effect of the reinforcement by three different geosynthetics on the shear strength of the Kilyos sand was evaluated. Initially the shear strength of the sand under various normal stresses were determined. Then, the effect of reinforcement was investigated. Based on the results obtained from the static tests, the effect of cyclic loads was investigated and the cyclic shear strength and strains were determined.

A. Materials

A poorly graded sand obtained from the Kilyos region in Istanbul, was used as the main material. Conducting the classification analysis, relative density test, and Pycnometer test, the engineering properties of the sand were obtained as presented in Table I.

A woven geotextile (G1) and two types of the geonets (G2 and G3) were used as the reinforcement geosynthetics. Since the dimensions of the existing geogrids were too big to be used in the small scale test, two types of geonets with various thickness and structures were used to simulate the three dimensional properties of geogrids. The reinforcement materials are shown in Fig. 1. The thickness of G1, G2, and G3 are 0.6, 1.3, and 3.8 mm respectively. Because of the small scale tests, the tensile strength of the geosynthetics were adequate enough to be assured that the shear failure of the soil will be occur prior to the tensile failure of the reinforcement materials. So, the tensile strengths of the geosynthetics were neglected.

TABLE I
Properties of Kilyos Sand

Soil type	**SP**
Effective size, D_{10} (mm)	0.25
Max. void ratio, e_{max}	0.77
Min. void ratio, e_{min}	0.44
Specific gravity	2.66
Plasticity index	Non-plastic

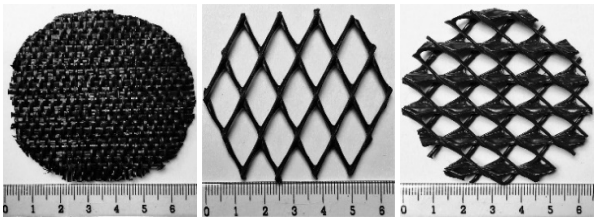

(a) (b) (c)

Fig. 1 Reinforcement materials; (a) woven geotextile (G1), (b) Geonet type 1 (G2), (c) Geonet type 2 (G3)

B. Testing Equipment

The static and cyclic simple shear tests were conducted using Geocomp ShearTrac II-DSS apparatus (Fig. 2). The tests were performed according to the standards ASTM D3080 [20] and ASTM D2435/T216 [21]. The testing system is capable of performing the consolidation, static and cyclic simple shear phases under full automatic control. Both stress and displacement controlled tests can be applied by the system. The application of cyclic loads is possible up to the maximum frequency of 1Hz under the simple shearing at a certain rate of deformation or force. An accuracy rate of displacement control can be performed from 0.00003 to 15 mm per minute. In this study, the static tests were conducted under displacement control applying the rate of 0.1 mm per minute. The testing system is able to measure and record axial vertical load, axial vertical displacement, axial horizontal load and displacement, and consequently volume change of the specimen [22].

C. Specimen Preparation

All tests were conducted with dry samples with the initial relative densities between 48% and 52%. The diameter for all specimens was 63.5 mm and considering different reinforcement materials, the sample heights ranged from 22.68 to 23.89 mm. As a common specimen preparation method for sands, dry funnel deposition (DFD) was used as shown in Fig. 3 [23]. The funnel containing sand was carefully raised along

the axis of symmetry of specimen allowing the sand particles into the specimen mold. Several samples were prepared to obtain the correct funnel height for preparing specimens at the desired density.

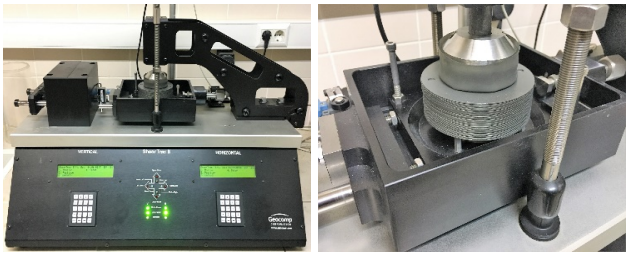

Fig. 2 Geocomp ShearTrac II-DSS apparatus

In the case of reinforced samples, one layer of the reinforcement material was implemented in the middle-height of the specimen. The middle-height of the specimens was determined by dividing the weight of whole sand in two parts, considering the amount of the sand which could be contained in openings of each utilized geosynthetic. Because of the different fabric structure of the reinforcement materials in various directions, some initial static and cyclic tests were conducted and the best reinforcement direction for each material was determined. Fig. 4 shows the installation of the reinforcement materials for both DSS and CSS tests where the shearing direction is horizontal.

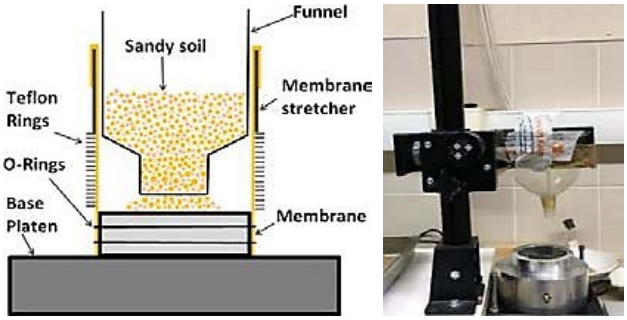

(a) (b)

Fig. 3 Specimen preparation using dry funnel deposition method: (a) schematic illustration of DFD method, (b) DFD method in laboratory

TABLE II
RESULTS OF STATIC SIMPLE SHEAR TESTS

Test ID	Sample	Prepared Sample		Compaction		Compacted Sample		Static Shear Phase		
		Height (mm)	DR (%)	Normal Stress (kPa)	Settlement (mm)	Height (mm)	DR (%)	Shear Rate (mm/min)	Max. Shear Strength (kPa)	Friction angle (degree)
DSS-S	Non-reinforced sand	22.83	51	150	0.7304	22.10	67	0.1	74	26
DSS-G1	Reinforced sand by G1	22.68	52	150	0.7491	21.93	70	0.1	78	28
DSS-G2	Reinforced sand by G2	22.86	52	150	0.8117	22.05	69	0.1	76	27
DSS-G3	Reinforced sand by G3	23.89	48	150	0.6283	23.26	61	0.1	80	28
DSS-S	Non-reinforced sand	22.75	52	225	0.6254	22.12	66	0.1	107	25
DSS-G1	Reinforced sand by G1	23.06	50	225	0.7628	22.30	66	0.1	120	28
DSS-G2	Reinforced sand by G2	23.35	49	225	0.9180	22.43	68	0.1	118	28
DSS-G3	Reinforced sand by G3	24.30	48	225	0.9495	23.35	67	0.1	122	28
DSS-S	Non-reinforced sand	22.82	51	300	0.8130	22.01	68	0.1	144	26
DSS-G1	Reinforced sand by G1	23.26	48	300	0.8030	22.46	65	0.1	160	28
DSS-G2	Reinforced sand by G2	23.35	49	300	0.9728	22.38	69	0.1	150	27
DSS-G3	Reinforced sand by G3	23.65	48	300	0.9035	22.75	67	0.1	152	27

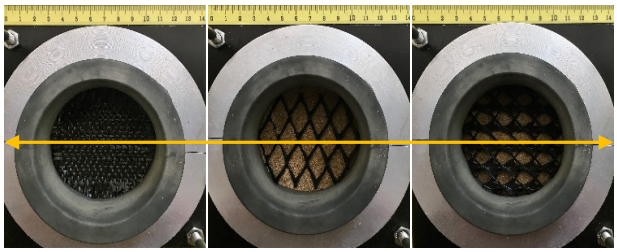

Fig. 4 Installation of the reinforcement materials

IV. TESTING PROGRAM

The testing program consists of two series of the experiments including direct simple shear test (DSS) cyclic simple shear test (CSS). A comprehensive experimental testing program conducted on non-reinforced and reinforced samples using three different reinforcement materials, including a woven geotextile and two types of geonet. In the both static and cyclic tests, the samples initially were confined horizontally and vertically and were compacted under the normal stresses of 150, 225 and 300 kPa. After applying the normal stresses, the relative density of the samples increased by the average amount of 16%. So, the shearing loads applied on the samples with the relative density of about 66%.

A. Direct Simple Shear Tests (DSS)

The Series 1 included the static direct simple shear tests. To provide a constant shear ratio and obtain more accurate results, displacement control tests were conducted with the displacement ratio of 0.1 mm per minute. 12 DSS tests were conducted on various non-reinforced and reinforced samples.

B. Results of the DSS Tests

According to the results shown in Table II, the inclusion of all three types of geosynthetics improves the shear strength. In addition, the friction angles also increase. From Fig. 5, it can

be concluded that by increasing the normal stress, the shear strength for sand increases almost linearly.

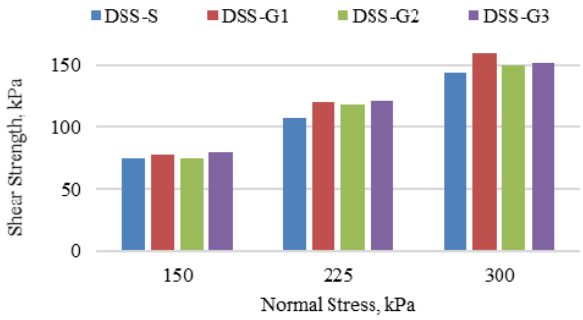

Fig. 5 Effect of reinforcement on static shear strength

According to the results, the maximum shear strength belongs to reinforced sample by G1 under the normal stress of 300 kPa. However, the maximum improvement of the shear strength was obtained for the reinforced sample by G3 under the normal stress of 225 kPa (DSS-G3-225) where 14% of the improvement achieved.

C. Cyclic Simple Sher Tests (CSS)

Due to the cyclic loads, excess pore water pressure generation and consequently liquefaction risk is a critical issue that should be considered. Hence, it is intended to investigate the effect of geosynthetic reinforcement on the number of load cycles which causes failure or undesired strains.

The cyclic loads were applied in the frequency of 1Hz and cycle period of 1 second, under the stress ratio amplitude of 0.30. The stress ratio amplitude (SRA) is defined as the ratio of the horizontal stress that is being applied in each cycle over initial vertical stress. All tests were conducted on the constant volume test concept which means the system gets feedback from real-time vertical and horizontal displacements and keeps the volume constant by adjusting the vertical load. It generates excess pressure in the sample. When the excess pressure becomes equal to the applied normal stress, the effective stress becomes zero and the sample liquefies. Therefore, despite the fact that the sample is dry and there is no water, the liquefaction can also be evaluated by this method. So considering the fact that if we are looking for the cyclic strength corresponded to a certain strain or looking for the cycle, which causes liquefaction, the desired cyclic strength can be obtained. For the used sand in this study, conducting several CSS tests revealed that the excess pressure becomes equal to the normal stress when the peak to peak (p-p) shear strain approaches 12%. Hence, this was taken as a threshold value for the CSS tests.

TABLE III
RESULTS OF CYCLIC SIMPLE SHEAR TESTS

Test ID	Sample	Prepared Sample		Compaction		Compacted Sample		Cyclic Shear Phase	
		Height (mm)	DR (%)	Normal Stress (kPa)	Settlement (mm)	Height (mm)	DR (%)	Stress Ratio Amplitude	Number of Cycles
CSS-S	Non-reinforced sand	22.75	52	150	0.97	21.78	73	0.3	84
CSS-G1	Reinforced sand by G1	22.92	49	150	0.92	22.00	69	0.3	121
CSS-G2	Reinforced sand by G2	23.28	49	150	0.87	22.41	67	0.3	144
CSS-G3	Reinforced sand by G3	23.80	48	150	1.06	22.74	69	0.3	48
CSS-S	Non-reinforced sand	22.85	50	225	0.94	21.91	70	0.3	194
CSS-G1	Reinforced sand by G1	23.01	48	225	1.09	21.92	71	0.3	230
CSS-G2	Reinforced sand by G2	23.10	50	225	0.98	22.12	71	0.3	287
CSS-G3	Reinforced sand by G3	23.80	48	225	1.04	22.76	69	0.3	105
CSS-S	Non-reinforced sand	22.86	50	300	0.98	21.88	71	0.3	270
CSS-G1	Reinforced sand by G1	23.15	49	300	1.22	21.93	75	0.3	230
CSS-G2	Reinforced sand by G2	23.15	49	300	1.07	22.08	72	0.3	368
CSS-G3	Reinforced sand by G3	23.71	49	300	1.24	22.47	75	0.3	175

D. The Results of the CSS Tests

12% of the p-p shear strain has been selected as the reference value for determining the number of cycles. The results from Table III show that for the samples under higher levels of normal stress, the mentioned strain occurs at the high number of load cycles. Fig. 6 shows that the failure occurs when the excess pore pressure becomes equal to the applied normal stress. This takes place around the cycles corresponding the 12% of the p-p shear strain. Both G1 and G2 are effective under cyclic loads and inclusion of G2 results in the maximum improvement on the number of cycles and increases it up to 71% (Test ID DSS-G2 with normal stress of 225 kPa from Table III). Unlike the static loads, G3 is not effective under cyclic loads.

Fig. 7 shows the output of the cyclic simple shear test on the sample CSS-G2. For the p-p shear strain of 12%, the liquefaction of the sample is visible when the excess pressure approaches to the applied normal stress of 225 kPa.

V. IMAGE PROCESSING ANALYSIS

An image processing analysis was conducted on the DSS tests to investigate the changes of the shear deformation profiles in the various non-reinforced and reinforced samples. The analysis is based on the *optical flow method* by using a MATLAB code. This method gives the motion pattern of the two consecutive frames caused by the movement of objects. It is a 2D vector field where each vector shows the direction of the movement of points between two frames. In this case, it

was aimed to obtain the lateral deformation profiles for 10 mm of the horizontal displacement. It should be mentioned that the shear failure of the samples occurred at the stains about 2%, but, to monitor the displacements clearly, the tests continued up to 10 mm of the horizontal displacement. For each DSS test, two photos were taken, the first one before starting the test with zero deformations, and the second one at the end of the test showing the final profile of the shear strains.

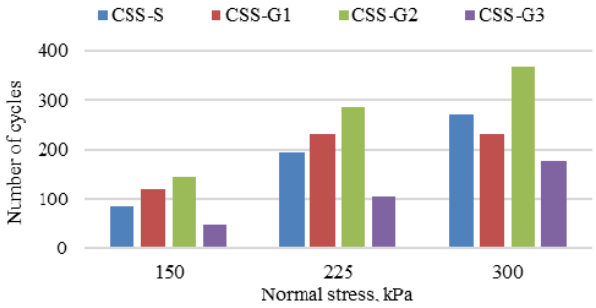

Fig. 6 Effect of reinforcement on cyclic shear strength

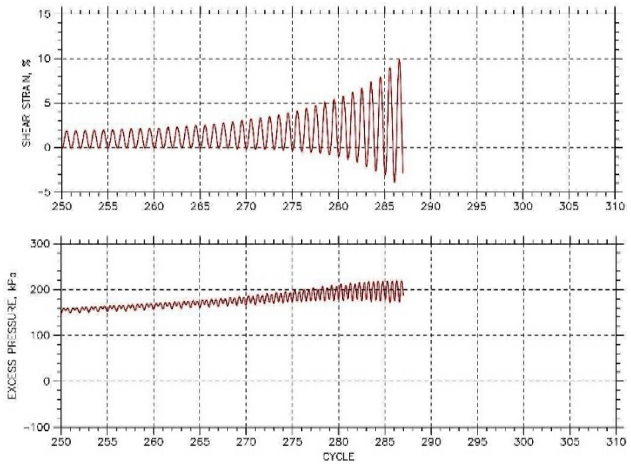

Fig. 7 Cyclic simple shear test

To conduct the image processing analysis, initially the camera stand was fixed at the level and perpendicular to the specimen. The camera calibration involves capturing the initial and deformed samples with a known distance of 20 mm on a white background. All photos were taken at the same resolution of 300 × 400 pixels. As it is shown for the test ID DSS-G3 in Fig. 8 (a), the vector fields of the motions were obtained by use of the Lucas-Kanade optical flow method. The direction and the number of the vectors shows the movement orientation and the concentration of the shear strains respectively. To make a comparison on the lateral displacement profiles between the initial and the sheared samples, the local distortions were obtained using a MATLAB code. Fig. 8 (b) shows the local distortion for the sample reinforced by G3.

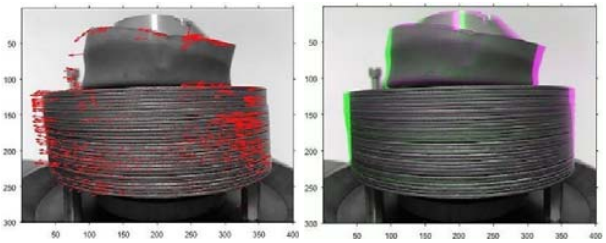

(a) (b)

Fig. 8 Image processing on the test ID DSS-G3 for the normal stress of 150 kPa; (a) vector field, (b) local distortion

Then, the coordinates of the pixels from the fixed and moving edges used to plot the shear strain profiles. Fig. 9 shows the shear strain profiles for the samples under the normal stress of 150 kPa.

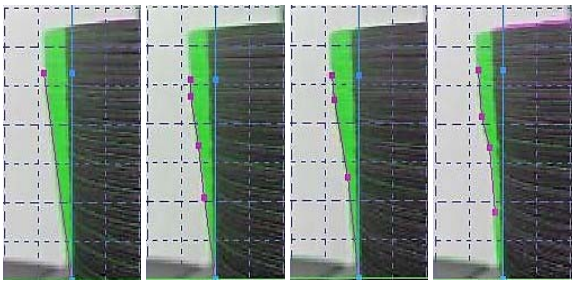

(a) (b) (c) (d)

Fig. 9 Shear strain profiles for normal stress of 150 kPa; (a) DSS-S, (b) DSS-G1, (c) DSS-G2, (d) DSS-G3

Fig. 10 illustrates a scheme of the height-displacement relation for non-reinforced and reinforced samples. It shows that how the reinforcement decreases the lateral displacements along the sample height. The maximum reduction occurs in the middle-height where the reinforcement is implemented.

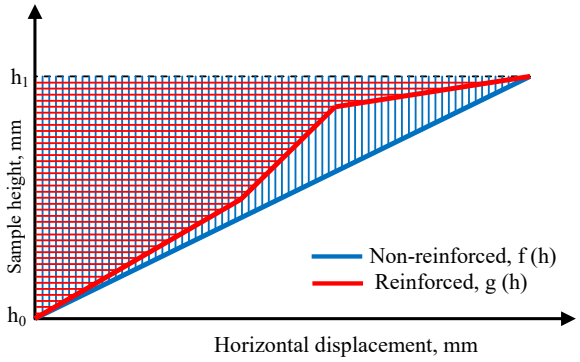

Fig. 10 Schematic illustration for shear strain profiles of the non-reinforced and reinforced samples

To investigate the effect of the reinforcement on the shear strain profiles, the area under the displacement curves along the height of the specimens calculated by (1) where h_1-h_0 is the height of the specimen and, f (h) and g (h) are the equations for the non-reinforced and reinforced samples respectively.

$$\int_{h_0}^{h_1}((f(h)-g(h))dh \quad (1)$$

The results of the image processing analysis approve that the reinforcement decreases the lateral displacements. Moreover, the applied normal stress is also effective on the lateral displacements and the bigger normal stress, the lower lateral displacements occurs. Fig 11 (a) shows how the various normal stresses affect the shear strain profile of the non-reinforced samples. The effect of the reinforcement on the samples under the normal stress of 150 kPa, is shown in Fig. 11 (b).

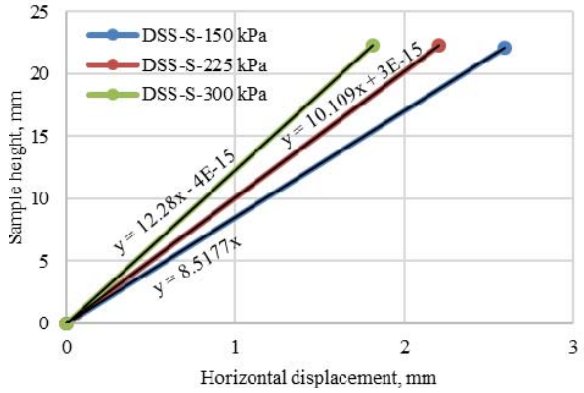

(a)

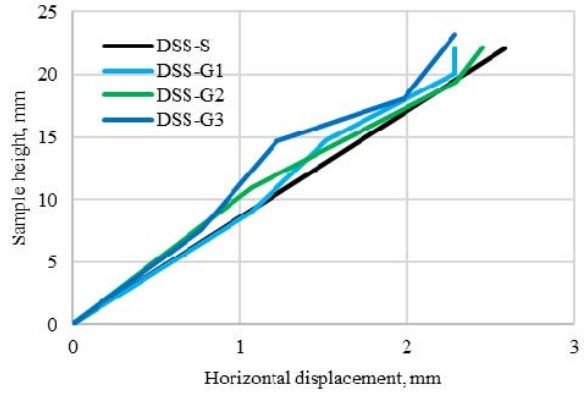

(b)

Fig. 11 Shear strain profiles; (a) non-reinforced samples under different normal stresses, (b) reinforced samples under the normal stress of 150 kPa

A comparison among the areas under the displacement curves reveals a reduction for the reinforced samples. Fig. 12 (a) shows a general descent manner in the way that the thicker reinforcement materials cause more reduction of displacements. The improvement percentages are presented in Fig 12 (b). According to the results, as a general behavior, the more thickness of the reinforcement material the more reduction on the lateral displacements occur.

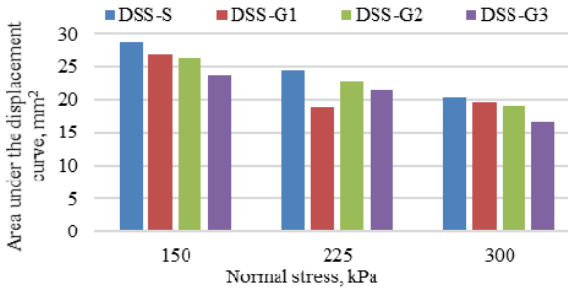

(a)

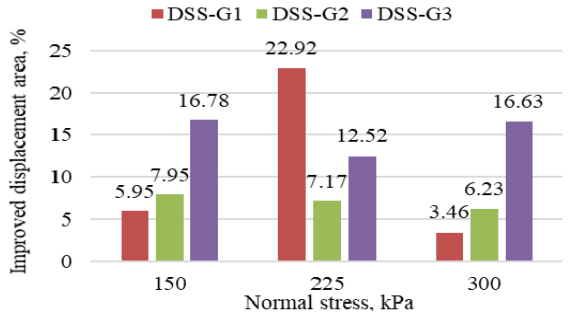

(b)

Fig. 12 Effect of reinforcement on shear strain reduction; (a) area under the lateral displacement curve along the height of the sample (b) percentage of the reduced displacement

VI. Conclusion

The effect of the geosynthetic reinforcement on the shear strength and shear strain profile of a poorly graded sand was investigated. Considering the main aim of the study as evaluation of the reinforcement effect on the lateral displacements and strain profiles, three different geosynthetics with various thicknesses were used as the reinforcement materials.

The static and cyclic shear strengths of the non-reinforced and reinforced samples were determined by conducting a series of direct simple shear and cyclic simple shear tests. In the case of the static tests, displacement control tests at the rate of 0.1 mm per minute were performed. Prior to each DSS or CSS test, the initial relative densities of the prepared samples were enhanced by applying a normal stress and keeping it at the shearing phase. Several tests were conducted applying the normal stresses of 150, 225, and 300 kPa. According to the results, for the higher level of normal stress, the higher shear strengths achieved under static and cyclic loads. All three types of the used geosynthetics were effective on the increase of the shear strength under the static loads. The maximum improvement was obtained a 14% increase of the shear strength. In the case of the cyclic tests, except the G3, the other two materials enhanced the shear strength and the most improvement was 71%. It can be said that the used reinforcement materials are more effective for improving shear strength under the cyclic loads rather than the static loads.

The variations of the shear strain profiles were investigated

by image processing analysis based on the optical flow method. Since the ending point of the CSS tests was not same for all cases, the image processing analysis was done only for the DSS tests. The results approve that, no matter the sample is reinforced or not, by increasing the normal stress, the lateral displacements decrease. Moreover, the reinforcement is also effective in decreasing shearing displacements. It is visible that the more thickness of reinforcement, the lower lateral displacements occur. The maximum improvement achieved by the reinforced sample with G1 (DSS-G1) under the normal stress of 225 kPa, where the displacement decreased by 22.92%. As a general idea, it can be concluded that the applied normal stress and the thickness of the reinforcement material can be considered as two main factors for reduction of the shear strains. The improved region and the spacing of the reinforcement materials, is an important factor that a proper and accurate determination of it can lead to a more economic and sustainable design. As a future work, considering the allowable shear strains, it is suggested that the optimized reinforcement spacing to be investigated. In the case of the cyclic tests, conducting video processing instead of the image processing would be beneficial.

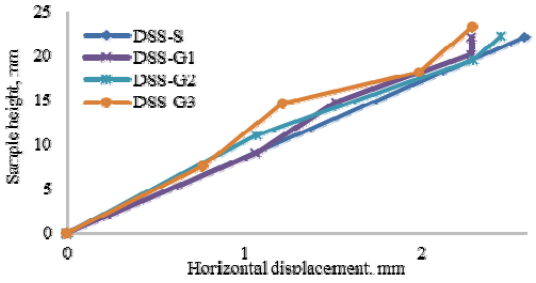

Fig. 13 Shear Strain Profiles, normal stress = 150 kPa

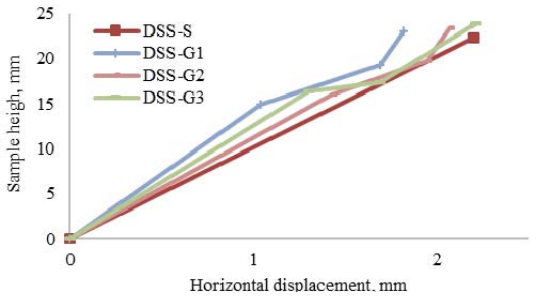

Fig. 14 Shear Strain Profiles, normal stress = 225 kPa

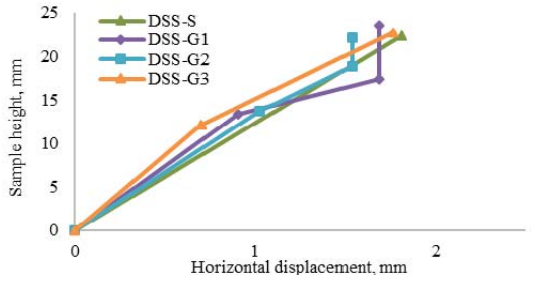

Fig. 15 Shear Strain Profiles, normal stress = 300 kPa

REFERENCES

[1] Y. Qian, et al., "Characterization of geogrid reinforced ballast behavior at different levels of degradation through triaxial shear strength test and discrete element modeling", *Geotextiles and Geomembranes* (2015), http://dx.doi.org/10.1016/j.geotexmem.2015.04.012.

[2] C.C.J. Kwan, "Geogrid Reinforcement of Railway Ballast". *Thesis submitted to the University of Nottingham for the degree of Doctor of Philosophy*, September 2006.

[3] E.C. Shin, D.H. Kim and B.M. Das, "Geogrid-reinforced railroad bed settlement due to cyclic load". *Geotechnical and Geological Engineering* (2002) 20: 261. doi:10.1023/A:1016040414725.

[4] G.P. Giroud, and J. Han, (2004). "Design method for geogrid-reinforced unpaved roads; I: Development of design method; II: Calibration and applications", *Journal of Geotechnical and Geoenvironmental Engineering, ASCE*, 130(8): 775-797.

[5] U.S. Army Corps of Engineers (2003). "Use of Geogrids in Pavement Construction". ETL 1110-1-189.

[6] E. Guler, S. K. Khosrowshahi. 2017 "Evaluation of the Geosynthetic Reinforcement on Railroad Subgrade". *Procedia Engineering,* Volume 189, Pages 721-728.

[7] A. K. Ashmawy, P. L. Bourrdeau, 1998. "Effect of geotextile reinforcement stress-strain and volumetric response of sand". *Proceeding of the Sixth International Conference on Geosynthetics*, Vol. 2, Atlanta, pp. 1079 – 1082.

[8] B. B. Broms, 1977. "Triaxial tests with fabric-reinforced soil. *Proceeding of the International Conference on the Use of Fabric in Geotechnics, Vol. 3, Ecole Nationale des Ponts et Chaussees, Paris.* pp. 129 – 134.

[9] R. Hufenus, R. Rueegger, R. Banjac, P. Mayor, S. M. Springman, R. Bronnimann, 2006. "Full-scale field tests on geosynthetic reinforced unpaved roads on soft subgrade". *Geotextiles and Geomembranes* 24 (1), 21–37.

[10] R. Ziaie Moayed, M. Nazari, "Effect of Utilization of Geosynthetic on Reducing the Required Thickness of Subbase Layer of a Two Layered Soil". *International Journal of Environmental, Chemical, Ecological, Geological and Geophysical Engineering* Vol:5, No:1, 2011.

[11] D. Penumadu, "Evaluating clay micro-fabric using scanning electron microscopy and digital information processing". *Transportation Research Record. No 1526, National Research Council.* Washington DC (1996). pp112-120.

[12] R. D. Hryciw, and S. A. Raschke, "Development of Computer Vision Technique for in Situ Soil Characterisation". *Transportation Research Record 1526. Transportation Research Board.* Washington (1996). pp86-97.

[13] B. Muhunthan, and J. Chameau, 1997. "Void fabric tensor and ultimate state surface of soils". *Journal Geotechnical and Geoenvironment Engineering. Volume 123, No 2*, pp173-181.

[14] E. Masad, B. Muhunthan, N. Shashidhar, and T. Harman, 1999. "Internal Structure Characterisation of Asphalt Concrete using Image Analysis". *Journal Computing Civil Engineering.* Volume 13, No 2, pp 88-95. USA (1999).

[15] D. Frost, and D. Jang, 2000. "Evolution of sand microstructure during shear". *Journal of Geotechnical and Geoenvironment Engineering.* Volume 126, No 22, New York, pp 116-130.

[16] K. Alshibli, and S. Sture, "Sand shear band thickness measurement by digital imaging techniques". *Journal of Geotechnical and Geoenvironmental Engineering.* Volume 13 No 2, pp 103-109. USA, 1999.

[17] K. Alshibli, and S. Sture, "Shear Band Formation in Plane Strain Compression". *Journal of Geotechnical and Geoenvironmental Engineering.* Volume 126, No 6, pp 495-503. USA, 2000.

[18] W. Harris, G. Viggiani, M. Mooney, and R. Finno, "Use of stereophotogrammetry to analyse the development of shear bands in sand". *Geotechnical Testing Journal.* Volume 18, No 4, pp 405-420. USA, 1995.

[19] R. Finno, W. Harris, M. Mooney, and G. Viggiani, "Shear Bands in Plane Strain Compression of Loose Sand". *Geotechnique.* Volume 47, No 1, pp 149-165. London 1997.

[20] ASTM D3080, Standard Test Method for Direct Shear Test of Soils under Consolidated Drained Conditions.

[21] ASTM D2435/T216, One-Dimensional Consolidation Properties of Soils.

[22] "Geocomp Product Specification for Shear Trac-II-DSS". http://www.geocomp.com/Products/TT_Cyclic_DSS.

[23] M. M. Monkul, Yamamuro, A. Jerry, 2010. "Influence of Densification Method on Some aspects of Undrained Silty Sand Behavior". International Conferences on Recent Advances in Geotechnical Earthquake Engineering and Soil Dynamics. 29.